# Composition depth profiling of polystyrene / poly(vinyl ethyl ether) blend thin films by angle resolved XPS.

G.Beamson[1]*, P.Mokarian-Tabari[2] and M.Geoghegan[2].

1. National Centre for Electron Spectroscopy and Surface Analysis (NCESS), STFC Daresbury Laboratory, Warrington, Cheshire. WA4 4AD, UK.
2. Department of Physics and Astronomy, University of Sheffield, Hounsfield Road, Sheffield. S3 7RH, UK.

* Corresponding author. Tel.: +44 1925 603 479; fax: +44 1925 603 596. *E-mail address:* graham.beamson@stfc.ac.uk.

**Keywords.**

Polystyrene, poly(vinyl ethyl ether), thin film polymer blend, angle resolved XPS, scanning force microscopy, composition depth profile.

**Abstract.**

Angle resolved XPS (ARXPS) and scanning force microscopy (SFM) are used to study polystyrene / poly(vinyl ethyl ether) 50 / 50 wt% blend thin films spin cast from toluene solution, as a function of polystyrene molecular weight and film thickness. ARXPS is used to investigate the composition depth profile (CDP) of the blend thin films and SFM to study their surface morphology and miscibility. The CDPs are modelled by an empirical hyperbolic tangent function with three floating parameters. These are determined by non-linear least squares regression, their uncertainties estimated and the curve fit residuals analysed to demonstrate that the hyperbolic tangent CDP is a satisfactory fit to the ARXPS data. Conclusions are drawn regarding the behaviour of the blend thin films as the thickness and polystyrene molecular weight are varied. Flory-Huggins interaction parameters ($\chi$) for the

mixtures are calculated based upon the segregation data, and suggest a value of $\chi$ = 0.05 to be appropriate for this system.

## 1. Introduction.

The behaviour of polymer blend thin films is often significantly different from that of the same materials in the bulk and is important in applications such as paints, adhesives, polymer based electronics and biocompatible coatings. Particular phenomena of interest are the preferential segregation of blend components to interfaces, phase separation, wetting/dewetting, film stability, pattern formation and thin film confinement effects [1-3]. Hence for both fundamental and applied reasons the surface and interface regions of polymer blend thin films have been studied intensively for many years using depth profiling and microscopy techniques. For example, neutron reflectometry [4] and MeV ion scattering [5] have been used to provide composition depth profile (CDP) information, and scanning force microscopy (SFM) has been used to study surface morphology [6-8]. Polymer blend thin films are often prepared by spin casting from solvent onto a suitable substrate, as this allows straightforward control of film thickness via solution concentration and rotation speed, and studied as a function of film thickness [9, 10] and molecular weight (MW) [11-13].

X-ray photoelectron spectroscopy (XPS) can provide elemental composition and chemical speciation information from the near surface region of a polymer sample [14-18] and when combined with ion sputtering can provide CDP information, although with reduced knowledge of chemical speciation due to the destructive nature of the sputtering process. Angle resolved XPS (ARXPS) can also be used to investigate the CDP of a sample between ~ 1 and ~ 8 nm of the uppermost surface [19-31] with less sample damage than caused by ion beam sputtering. The physics of the ARXPS method has been outlined in several publications [32-

34] and Cumpson [35] has shown how uncertainties in the intensity measurements limit the information that can be extracted from the data. The measured photoelectron intensity from a particular core level of a particular species is given by [20]:

$$I(\theta) = K\sigma F \int_0^\infty c(z).\ \exp(-z / \lambda\sin\theta).\ dz \qquad (1)$$

K is the product of various instrumental factors, $\sigma$ is the photoionization cross-section, F is the spectrometer transmission, c(z) is the concentration of the species as a function of depth z, i.e. the CDP, $\lambda$ is the photoelectron inelastic mean free path and $\theta$ is the photoelectron take-off-angle measured relative to the sample surface. A set of angle resolved XPS data consists of measurements of $I(\theta)$ at several values of $\theta$, typically between 5 and 10, and recovery of c(z) amounts to taking the inverse Laplace transform of the angle resolved data set. This can be achieved numerically but the problem is fundamentally "ill-conditioned" and very sensitive to noise in the data, i.e. to the uncertainties in the intensity measurements. For realistic signal / noise ratios of ~ 100 only three parameters relating to the CDP can be reliably extracted from the data [35]. Thus care needs to be exercised in the interpretation of CDP parameters determined from ARXPS and estimates made of the uncertainties in those parameters. A number of methods are available for carrying out the inverse Laplace transform but it is generally accepted that the best procedure is to use the least squares method to fit a model of the CDP based on prior knowledge to the experimental ARXPS data [24, 27, 33, 35].

Here we describe a study of polystyrene / poly(vinyl ethyl ether) (PST / PVEE) blend thin films as a function of PST MW and film thickness. PST / PVEE blends are chemically similar to the

much studied polystyrene / poly(vinyl methyl ether) (PST / PVME) blend system [29-31, 36-39] but with a less favourable Flory-Huggins interaction parameter. (The Flory-Huggins interaction parameter, usually denoted $\chi$, is a dimensionless and temperature-dependent measure of the interaction energy between two components relative to their energies in their own melts. The $\chi$-parameter, along with the MWs of the chains is all that is needed to define the miscibility of a polymer blend at a given composition using the regular solution theory of polymer mixtures [40].) This has been attributed to greater shielding of the interaction between the ether oxygen atom and the aromatic ring by the ethyl group of PVEE compared with the methyl group of PVME [41]. The less favourable interaction causes PST / PVEE blends to change from miscible to phase separated as the PST MW increases. PVEE preferentially segregates to the blend surface and we describe the use of ARXPS to investigate the CDPs of the blend thin films and of SFM to study their surface morphology and hence miscibility. We assume that the CDPs can be modelled by an empirical hyperbolic tangent function [42] described by three floating parameters. These are determined by non-linear least squares regression, their uncertainties estimated and the curve fit residuals analysed to demonstrate that the hyperbolic tangent CDP is a satisfactory fit to the ARXPS data. Conclusions are drawn regarding the behaviour of the blend thin films as the thickness and PST MW are varied and Flory-Huggins interaction parameters are calculated for each film, based upon the CDP.

Systematic uncertainties often dominate random ones in determining the accuracy of an XPS analysis [35, 43] and we describe steps taken to minimise the effect of x-ray induced sample damage [44] during our experiments and to investigate the effect of contaminants present in the PST / PVEE samples. Another important experimental consideration when carrying out an

ARXPS study of an electrically insulating polymer sample is the need to maintain good charge compensation, and hence spectral resolution, as $\theta$ is varied.

## 2. Experimental.

The x-ray photoelectron spectra were recorded using a Scienta ESCA300 spectrometer. This employs a high power rotating anode and monochromatised Al K$\alpha$ x-ray source ($h\nu$ = 1486.7 eV), high transmission electron optics and a multichannel detector [45, 46]. The geometry of the x-ray source, sample manipulator and electrostatic lens is such that at low $\theta$ the x-ray beam strikes the sample at glancing incidence. This gives enhanced sensitivity at low $\theta$ and is ideal for the study of thin film samples [45]. The $\theta$ scale of the spectrometer was calibrated by recording Si 2p spectra of a piece of silicon wafer as a function of the angle setting of the sample manipulator and measuring the angle at which the Si(0)/Si(IV) ratio was a maximum, which corresponds to $\theta = 90^{o}$. For C 1s photoelectrons and the instrument settings used in this work the angular acceptance of the ESCA300 lens is ~ +/- $3^{o}$ [47]. The energy scale of the spectrometer was regularly checked using the Fermi edge, $3d_{5/2}$ and $M_4VV$ lines of a sputter cleaned sample of silver foil, and the measured binding energies came within 0.1 eV of the corresponding literature values (0.0, 368.26 and 1128.78 eV respectively) [48]. Spectra were recorded at 150 eV pass energy and 0.8 mm slit width, giving an overall instrument resolution of ~ 0.35 eV [49]. The x-ray source power was 2.8 kW and charge compensation was achieved using a Scienta FG300 low energy electron flood gun. The step interval of the region spectra was 0.05 eV.

Details of the polymers used for preparation of the blend thin films are shown in Table 1. All the polymers were obtained from Aldrich and used as received from the supplier. For each PST / PVEE MW combination, 50 / 50 wt% mixtures, 0.5 - 10 wt% in toluene, were made by

accurate weighing into clean glass vials. Solutions of pure PST and pure PVEE, ~ 3 wt% in toluene, were also prepared. One drop of solution was placed on a 10 mm diameter glass disk (wiped with tissue / isopropanol) fixed with double sided tape to an XPS sample stub and mounted on a spin coater. After spinning for ~ 30 seconds at 2000 rpm the samples were transferred immediately to the vacuum system of the XPS spectrometer. For each blend solution a first spin cast sample was used to record a survey spectrum at $\theta = 90^o$ and a second, fresh sample, was used to record a sequence of C 1s spectra at $\theta = 90^o$, $75^o$, $60^o$, $45^o$, $30^o$, $20^o$ and $10^o$. The sample position was changed systematically between the C 1s spectra, both to minimise the effect of x-ray induced sample damage and for optimum charge compensation. The acquisition time for each C 1s spectrum was ~ 2.5 minutes and the effect of x-ray induced damage on the angle resolved spectra is judged to have been small.

Calibration curves of the PST / PVEE blend film thickness as a function of the concentration of the toluene solution used for spin casting were generated by spin casting onto silicon wafer substrates at 2000 rpm and measuring the absorbance of the PST 700 $cm^{-1}$ line using a Bio-Rad FTS-60A FTIR spectrometer. The relationship between absorbance and film thickness was determined by placing a scratch across several pure polystyrene thick film samples and measuring the depth of the scratch using a step profilometer.

SFM images of blend films on silicon wafer substrates were recorded using a Nanoscope IIIa (Veeco, Santa Barbara, USA) operated in tapping mode with an OMCL silicon probe from Olympus. The cantilevers had a nominal spring constant of 40 N / m and a resonant frequency of 300 kHz. Height and phase data were collected simultaneously and the images were analysed using Nanoscope software, version 5.12.

Thick drop cast films of the PST / PVEE blends were prepared for visual observation of phase separation by placing several drops of ~ 10 wt% solution in toluene onto 10 mm diameter glass disk substrates and leaving to dry in air for 2 days. These films are estimated to have been several hundred microns thick.

**3. Data Analysis.**

The C 1s spectra of pure PST and PVEE are shown in Figure 1 and a set of angle resolved C 1s spectra for a thin film blend sample is shown in Figure 2. The pure PST spectrum is shown binding energy referenced to C 1s = 284.8 eV and the PVEE spectrum to the lowest binding energy C 1s component = 285.0 eV. This brings the second component of the PVEE spectrum to 286.4 eV, in agreement with previous measurements [14], and the spectra shown in Figure 2 are binding energy referenced to this value.

For each angle resolved data set (consisting of C 1s spectra at 7 values of $\theta$) the areas of the PST and PVEE spectra ($A(\theta)_{PST}$ and $A(\theta)_{PVEE}$) present in the blend spectra were determined by curve fitting using CasaXPS software [50], with spectra of the pure PST and PVEE films as basis functions. A typical curve fit is shown in Figure 3. The experimental PVEE apparent volume fractions were calculated from:

$$\phi(\theta)_{Expt} = \frac{A(\theta)_{PVEE}}{A(\theta)_{PVEE} + A(\theta)_{PST} \times (M_{PST} / M_{PVEE}) \times (4/8) \times (\rho_{PVEE} / \rho_{PST})} \quad (2)$$

$M_{PVEE}$ and $M_{PST}$ are the repeat unit molecular weights (72 and 104 Da respectively), 4 / 8 is the ratio of the number of carbon atoms in the PVEE / PST repeat units and $\rho_{PVEE}$ and $\rho_{PST}$ are the polymer densities (0.968 and 1.047 g/cm$^3$ respectively).

For a binary polymer blend in which one component preferentially segregates to the surface the CDP in the near surface region, expressed in terms of the volume fraction of the surface segregating component, $\phi(z)$, can be described by an empirical hyperbolic tangent function [42]:

$$\phi(z) = \phi_b + (\phi_s - \phi_b).\frac{(1 - \tanh((z - \Delta)/\sigma))}{(1 - \tanh(-\Delta/\sigma))} \qquad (3)$$

$\phi_s$ and $\phi_b$ are the surface and bulk volume fractions, $\Delta$ is related to the thickness of the surface overlayer (essentially providing a parameter to replicate flattening of the CPD near the surface [51]) and $\sigma$ determines the width of the interface region between the surface and the bulk; see Figure 4. In PST / PVEE blends PVEE segregates to the surface because of its lower surface free energy and we assume that $\phi_s$ for PVEE is one. This is supported by the ARXPS data but we note that because the minimum XPS sampling depth (i.e. $3\lambda\sin\theta$ at $\theta$ = 10$^o$) is ~ 2 nm, the assumption may not be strictly true for all the blend thin films.

Hence, with the CDP of equation (3) PVEE apparent volume fractions can be calculated from:

$$\phi(\theta)_{Calc} = \int_0^t \phi(z).\exp(-z / \lambda\sin\theta).dz \Big/ \int_0^t \exp(-z / \lambda\sin\theta).dz \qquad (4)$$

Within an Excel 2003 spreadsheet trial initial values of $\phi_b$, $\Delta$ and $\sigma$ were used to calculate $\phi(z)$ from equation (3) and then $\phi(\theta)_{Calc}$ at each of the experimental $\theta$ values by numerical integration of equation (4). For films thicker than 20 nm the upper limit of the integration, t, was set equal to 20 nm, whereas for thinner films it was set equal to the film thickness. For all films dz = t/1000. For C 1s photoelectrons excited by Al K$\alpha$ radiation moving through PST / PVEE $\lambda$ was taken as 3.7 nm [52]. This model neglects elastic scattering effects which have been shown to be small for PST [20].

The final values of $\phi_b$, $\Delta$ and $\sigma$ were determined by minimisation of the sum of square differences: $\Sigma(\phi(\theta)_{Expt} - \phi(\theta)_{Calc})^2$ (i.e. summed over the 7 experimental $\theta$ values) using the Solver non-linear optimisation routine [53]. The standard deviations of $\phi_b$, $\Delta$ and $\sigma$ and the coefficient of determination, $R^2$, were calculated using the Solvstat macro [54]. This is equivalent to using the curve fit residuals to calculate the uncertainties in the CDP parameters, as discussed by Cumpson [35].

The curve fit values of $\phi_b$, $\Delta$ and $\sigma$ were used to calculate angle resolved profiles from equations (3) and (4) for comparison with the experimental data points, as shown in Figures 5a), 6a) and 7a). For one data set, out of the total of 18, comparison of the experimental points and the curve fit line revealed an obvious single outlier point; this was eliminated and Solver + Solvstat re-run. For four other data sets, where the range of $\phi(\theta)$ on going from $\theta$ = 90$^o$ to 10$^o$ was small, Solver produced low and obviously erroneous values for $\phi_b$, and in these cases it was fixed at a more appropriate value (see Section 4.2) and Solver + Solvstat re-run.

For each angle resolved data set the residual at each data point was calculated from:

$$\frac{\phi(\theta)_{Expt} - \phi(\theta)_{Calc}}{\phi(\theta)_{Calc}} \qquad (5)$$

and the mean and standard deviation of the residuals calculated for the data set.

To simulate the effect of different levels of noise in the experimental data a hyperbolic tangent composition depth profile with defined values of $\phi_b$, $\Delta$ and $\sigma$ was used to calculate $\phi(\theta)$ at $\theta$ = 90°, 75°, 60°, 45°, 30°, 20° and 10°, and random noise added to the data points such that the standard deviation of the noise was equal to a certain fraction of $\phi(\theta)$, e.g. 0.5%. Solver was then used to re-calculate the values of $\phi_b$, $\Delta$ and $\sigma$, and the procedure repeated 10 times in order to obtain standard deviations for the re-calculated values.

## 4. Results and discussion.

### 4.1 SFM.

Thick drop cast samples of PST / PVEE blends are transparent for PST MW = 0.8 and 2.5 kDa and opaque for PST MW >= 4.1 kDa. The SFM data (Figure 8) reveal that for spin cast blend films ~ 100 nm thick only those with PST MW = 289 kDa have a rough surface topography (RMS roughness ~ 11.7 nm) indicating that they are phase separated, the surfaces of the other films being rather smooth (RMS roughness ~ 0.3 - 0.8 nm) indicating that they are miscible. In addition, spin cast films with PST MW = 289 kDa become smooth when the thickness is reduced to 30 and 12 nm (RMS roughness ~ 0.5 nm). For an incompatible polymer blend system ($\Delta H_{mix} > 0$) the reduction in the entropy of mixing ($\Delta S_{mix}$) with increasing MW causes $\Delta G_{mix} = \Delta H_{mix} - T\Delta S_{mix}$ (where T is the absolute temperature) to

become positive above a certain MW and phase separation to occur rather than mixing [3]. For the thick drop cast samples this transition is between PST MW = 2.5 and 4.1 kDa, whereas for the ~ 100 nm spin cast films it is between 19.3 and 289 kDa. Hence confinement of the PST / PVEE blends in thin film geometry appears to shift the transition from miscible to immiscible to higher MW. Similar thin film confinement effects have been observed in other polymer blend systems [6, 55-59]. On the basis of the SFM data we propose that the spin cast blend thin films with PST MW = 0.8, 2.5 and 4.1 kDa are miscible and that their angle resolved C1s data can be analysed using a hyperbolic tangent composition depth profile as described in section 3. The spin cast blend thin films with higher PST MW are either immiscible (289 kDa) or close to immiscible (19.3 kDa) and analysis of their angle resolved C 1s data is omitted.

**4.2 XPS.**

In addition to C and O the survey spectra of some of the thicker blend films spin cast onto glass substrates show a very low level of Si (~0.1 at% for films spin cast from ~ 10 wt% solutions in toluene, i.e. ~ 250 nm thick) probably due to the surface segregation of silicone contamination present in the bulk of the films. Interestingly, survey spectra of thick drop cast samples (many hundreds of microns thick) reveal significant Si contamination, e.g. ~ 5 at% for the blend with PST Mw = 4.1 kDa. This shows that although silicone contamination is present in the blends at rather low overall concentration the thick drop cast films contain enough material to give a high surface concentration of Si. However, for the spin cast films of interest here the film thicknesses are sufficiently small that the surface concentration of Si is almost undetectable. The survey spectra of blend films spin cast from dilute solutions in toluene, i.e. < 1 wt%, show C and O from the blend and Si from the glass substrate, with Si < 1 at%.

The experimental and curve fit angle resolved profiles for blends with PST MW = 0.8, 2.5 and 4.1 kDa are shown in Figures 5a), 6a) and 7a) and the corresponding composition depth profiles in Figures 5b), 6b) and 7b). The curve fit values of $\phi_b$, $\Delta$ and $\sigma$, together with their standard deviations are shown in Table 2. With one exception (for which the value is 0.98) the $R^2$ values for the curve fits are > 0.99, the mean of the residuals is in the range -0.07 - 0.02% and their standard deviations are in the range 0.34 to 1.42%. Taking the 18 datasets together gives the mean and standard deviation of the residuals as -0.01% and 0.78% respectively, and plotting the residuals as a histogram gives a good approximation to a normal distribution. If the uncertainty in the curve fit parameters is taken as two standard deviations (95% confidence interval) the data show that in general $\phi_b$ and $\Delta$ are better determined than $\sigma$. This was confirmed by the simulations described at the end of Section 3, which also show that parameter standard deviations comparable with those in Table 2 are obtained with a simulated noise level of ~ 0.5 - 1.0%. Estimation of the uncertainties in $A(\theta)_{PST}$ and $A(\theta)_{PVEE}$ (equation (2)) using the Monte Carlo routine in CasaXPS gave standard deviations for $\phi(\theta)_{Expt}$ of ~ 0.4 - 0.7%. Thus both methods indicate that the experimental noise level is comparable to the standard deviation of the residuals for all the data sets. Values of $R^2$ close to one, and a normally distributed pattern of residuals with mean close to zero and standard deviation close to the experimental noise indicate that the model (i.e. the hyperbolic tangent CDP) used to calculate the angle resolved profiles is a satisfactory fit to the data [60].

The value of $\phi_b$ expected from the composition of the spin casting solutions is 0.52 +/- 0.01 and for thicker films of the PST(0.8 kDa) and PST(2.5 kDa) blends the curve fit values are well within two standard deviations of this. For one of the thicker PST(2.5 kDa) blend films and three of the PST(4.1 kDa) films it was necessary to constrain $\phi_b$ to be 0.52 otherwise

Solver produced low values for $\phi_b$ that are obviously erroneous. This constraint is justified by the observed trends in $\phi_b$ with thickness and PST MW. For all the PST MWs $\phi_b$ for the thinner blend films is noticeably less than 0.52, which may partly be due to there being insufficient material in such thin films to maintain both a surface excess of PVEE and $\phi_b$ ~ 0.52. The nature of any preferential segregation at the glass interface will also influence $\phi_b$ for the thinner blend films. The thickness of the surface overlayer, $\Delta$, is ~ 0.0 nm for all but the thinnest of the PST(0.8 kDa) blend films and increases to between 1.8 and 2.1 nm for the PST(2.5 kDa) films and between 2.9 and 3.5 nm for the PST(4.1 kDa) films. This development of a surface overlayer of PVEE (i.e. a wetting layer) reflects both the increase in the surface energy of PST with MW [30], which will reduce its concentration in the near surface region, and the tendency towards phase separation as the PST MW increases. For the two thinnest PST(0.8 kDa) blend films, i.e. the 15 and 10 nm films, the $\Delta$ values are somewhat larger than for the thicker films, which may represent a change in the film morphology, e.g. phase separation, as has been observed for very thin films of PST / PVME miscible blends [37].

Because a steep concentration gradient in the interface region between the surface and the bulk would restrict the number of conformations available to the polymer chains (hence reducing the entropy and increasing the free energy) the distance over which the surface concentration returns to the bulk value must be comparable with the size of the chains [3]. The radius of gyration of a polymer chain is given by [40]:

$$R_g = (Nb^2/6)^{0.5} \qquad (6)$$

N is the degree of polymerisation (the average number of monomer units per chain) and b is the average statistical segment length. For PST b = 0.68 nm and for PVEE we assume that it

is the same as for PVME, i.e. 0.69 nm [37]. Hence for the PSTs with MW = 0.8, 2.5 and 4.1 kDa $R_g$ = 0.8, 1.4 and 1.8 nm respectively, and for PVEE(3.8 kDa) $R_g$ = 2.0 nm. For the PST(0.8 kDa) blend films $\sigma$ falls in the range 1.0 - 1.8 nm (except for the thinnest film where $\sigma$ ~ 0.5 nm), increasing to 1.2 - 3.1 nm for the PST(2.5 kDa) films and 1.6 - 2.9 nm for the PST(4.1 kDa) films. Thus although the uncertainties in $\sigma$ are rather large the values are comparable with the radii of gyration of the PST and PVEE polymer chains.

**4.3 Calculation of the interaction parameter.**

Given the CDP of a polymer blend it is possible to obtain both the surface energy difference between the two components and the Flory-Huggins interaction parameter, $\chi$. The surface energy difference [2] requires accurate values of the surface volume fraction, and also that they are not close to unity, a condition that is not satisfied in the current work. The surface excess, z*, however, can be used to calculate the $\chi$ parameter. The surface excess is given by [2]:

$$z^* = \int_0^{\infty} (\phi(z) - \phi_b).\, dz = \frac{b(k_bT)^{0.5}}{6} \int_{\phi_s}^{\phi_b} \frac{(\phi - \phi_b).\, d\phi}{(G(\phi) - G(\phi_b) - \phi(1-\phi)(\delta G/\delta\phi)_{\phi_b})^{0.5}} \qquad (7)$$

where:

$$\frac{G(\phi)}{k_bT} = \frac{\phi \ln\phi}{N_{PVEE}} + \frac{(1-\phi)\ln(1-\phi)}{N_{PST}} + \chi\phi(1-\phi) \qquad (8)$$

is the free energy per lattice site and $N_{PVME}$ and $N_{PST}$ are the number of monomer units per PVEE or PST chain. It is therefore a straightforward matter to solve equations (7) and (8) numerically for $\chi$. Because the volumes occupied by the monomer units of PST (0.165 $nm^3$) and PVEE (0.124 $nm^3$) are different a lattice must be defined based upon one monomer unit of PST, which means that in equation (8) the PVEE chain length is taken as $N_{PVEE}$ = 39.5

monomer units rather than 3800/72 = 52.8. The values of $\chi$ obtained are tabulated in Table 2, and are seen to be molecular weight, but not thickness dependent. The thickness independence of $\chi$ suggests that the samples may be close to equilibrium. However, we recall that spin coating does not generally produce equilibrium structures and note that the thinnest films may be forced out of equilibrium by confinement effects. The dependence on the PST molecular mass may well be due to the small molecular weights used here, or it could indicate that the final blends are not actually in equilibrium. It is worth noting that the PST(4.1 kDa) / PVEE(3.8 kDa) blend system is symmetric because $N_{PST}$ = 39.4. Given the tendency of $\chi$ to decrease with increasing molecular mass, the best estimate for $\chi$ under the experimental conditions used is 0.05±0.01.

**Conclusions.**

Imaging of surface topography by SFM has shown that for PST / PVEE 50 / 50 wt% spin cast blend films, ~ 100 nm thick, the transition from miscible to phase separated shifts to a higher PST MW compared with the bulk, i.e. from between 2.5 and 4.1 kDa to above 19.3 kDa. We attribute this to a confinement induced miscibility effect similar to that observed in other polymer blend systems. ARXPS has been used to investigate the CDPs of the blend films for PST MWs of 0.8, 2.5 and 4.1 kDa and for film thicknesses between 15 and 300 nm. The CDPs were modelled with an empirical hyperbolic tangent function with $\phi_b$ (PVEE bulk volume fraction), $\Delta$ (surface overlayer thickness) and $\sigma$ (width of interface between surface overlayer and bulk) as floating parameters. Non-linear least squares regression was used to determine $\phi_b$, $\Delta$ and $\sigma$, and analysis of residuals was used to determine their uncertainties and to demonstrate that the hyperbolic tangent function provides a satisfactory fit to the ARXPS data. In general $\phi_b$ and $\Delta$ are better determined than $\sigma$, in agreement with the observation by

Paynter [34] that interface widths are less well determined from ARXPS measurements than layer concentrations and thicknesses. However, when a layer lies close to the limit of the XPS sampling depth (i.e. $3\lambda$) ARXPS can give an unreliable value for its concentration [34], as observed here, where for some of the thicker blend films it was necessary to fix $\phi_b$ at the known value of the bulk concentration during the least squares regression in order to avoid an obviously erroneous result.

For all the blends studied $\phi_b \sim 0.52$ for the thicker films and decreases with film thickness. This may be due, in part, to there being insufficient material in the thinner films to maintain both a surface excess of PVEE and $\phi_b \sim 0.52$. The value of $\Delta$ is ~ 0.0 nm for those blends with PST MW = 0.8 kDa and increases to ~ 2 nm and ~ 3 nm for those with PST MW = 2.5 and 4.1 kDa respectively. This is interpreted as due to the development of a surface overlayer of PVEE as the surface energy of the PST increases and as the system tends towards phase separation. The width of the interface between the surface overlayer and the bulk is ~ 1 - 3 nm and comparable with the radii of gyration of the polymer chains, as expected from simple thermodynamic arguments. The Flory-Huggins interaction parameter has been calculated using simple mean field theory and is given as $\chi = 0.05 \pm 0.01$ based upon a lattice with volume 0.165 $nm^3$.

**Acknowledgement.**

The UK Engineering and Physical Sciences Research Council (EPSRC) is acknowledged for financial support of NCESS under grants GR/S14252/01 and EP/E025722/1.

**References.**

[1] H.Wang, R.J.Composto, Phys. Rev. E 61 (2000) 1659.

[2] M.Geoghegan, G.Krausch, Prog. Polym. Sci. 28 (2003) 261.

[3] R.A.L.Jones, R.W.Richards, Polymers at Surfaces and Interfaces, CUP, 1999.

[4] R.A.L.Jones in: R.W.Richards, S.K.Peace (Eds.), Polymer Surfaces and Interfaces III, John Wiley, Chichester, 1999, 149.

[5] M.Geoghegan in: R.W.Richards, S.K.Peace (Eds.), Polymer Surfaces and Interfaces III, John Wiley, Chichester, 1999, 43.

[6] S.Zhu, Y.Liu, M.H.Rafailovich, J.Sokolov, D.Gersappe, D.A.Winesett, H.Ade, Nature 400 (1999) 49.

[7] C.Ton-That, A.G.Shard, R.H.Bradley, Polymer 43 (2002) 4973.

[8] P.Wang, J.T.Koberstein, Macromolecules 37 (2004) 5671.

[9] A.Hariharan, S.K.Kumar, M.H.Rafailovich, J.Sokolov, X.Zheng, D.Duong, S.A.Schwarz, T.P.Russell, J. Chem. Phys. 99 (1993) 656.

[10] G.Krausch, C.-A.Dai, E.J.Kramer, J.F.Marko, F.S.Bates, Macromolecules 26 (1993) 5566.

[11] M.Geoghegan, F.Abel, Nucl. Instrum. Meth. B 143 (1998) 371.

[12] M.Geoghegan, H.Ermer, G.Jüngst, G.Krausch, R.Brenn, Phys. Rev. E 62 (2000) 940.

[13] A.Hariharan, S.K.Kumar, T.P.Russell, J. Chem. Phys. 98 (1993) 4163.

[14] G.Beamson, D.Briggs, High Resolution XPS of Organic Polymers. The Scienta ESCA300 Database, John Wiley, Chichester, 1992.

[15] G.Beamson, D.T.Clark, N.W.Hayes, D.S.-L.Law, V.Siracusa, A.Recca, Polymer 37 (1996) 379.

[16] G.Beamson, B.T.Pickup, W.Li, S.-M.Mai, J. Phys. Chem. B 104 (2000) 2656.

[17] G.Beamson, M.R.Alexander, Surf. Interface Anal. 36 (2004) 323.

[18] G.Beamson, J. Electron Spectrosc. Relat. Phenom. 154 (2007) 83.

[19] Z.Chanbi, R.W.Paynter, J. Electron Spectrosc. Relat. Phenom. 164 (2008) 28.

[20] R.W.Paynter, D.Roy-Guay, G.Parent, M.Menard, Surf. Interface Anal. 39 (2007) 445.

[21] R.W.Paynter, M.Menard, J. Electron Spectrosc. Relat. Phenom. 151 (2006) 14.

[22] M.Menard, R.W.Paynter, Surf. Interface Anal. 37 (2005) 466.

[23] R.W.Paynter, H.Benalia, J. Electron Spectrosc. Relat. Phenom. 151 (2004) 209.

[24] R.W.Paynter, J. Electron Spectrosc. Relat. Phenom. 135 (2004) 183.

[25] R.W.Paynter, Surf. Interface Anal. 27 (1999) 103.

[26] S.Oswald, F.Oswald, Surf. Interface Anal. 40 (2008) 700.

[27] S.Oswald, M.Zier, R.Reiche, K.Wetzig, Surf. Interface Anal. 38 (2006) 590.

[28] M.Kozlowska, R.Reiche, S.Oswald, H.Vinzelberg, R.Hubner, K.Wetzig, Surf. Interface Anal. 36 (2004) 1600.

[29] D.H-K.Pan, W.M.Prest, J. Appl. Phys. 58 (1985) 2861.

[30] Q.S.Bhatia, D.H.Pan, J.T.Koberstein, Macromolecules 21 (1988) 2166.

[31] C.Forrey, J.T.Koberstein, D.H.Pan, Interface Sci. 11 (2003) 211.

[32] C.S.Fadley, R.J.Baird, W.Siekhaus, T.Novakov, S.A.L.Bergstrom, J. Electron Spectrosc. Relat. Phenom. 4 (1974) 93.

[33] J.Diao, D.W.Hess, J. Electron Spectrosc. Relat. Phenom. 135 (2004) 87.

[34] R.W.Paynter, J. Electron Spectrosc. Relat. Phenom. 169 (2009) 1.

[35] P.J.Cumpson, J. Electron Spectrosc. Relat. Phenom. 73 (1995) 25.

[36] K.El-Mabrouk, M.Belaiche, M.Bousima, J. Coll. Interface Sci. 306 (2007) 354.

[37] K.Tanaka, J-S.Yoon, A.Takahara, T.Kajiyama, Macromolecules 28 (1995) 934.

[38] A.Karim, T.M.Slawecki, S.K.Kumar, J.F.Douglas, S.K.Satija, C.C.Han, T.P.Russell, Y.Liu, R.Overney, J.Sokolov, M.H.Rafailovich, Macromolecules. 31 (1998) 857.

[39] D.Kawaguchi, K.Tanaka, T.Kajiyama, A.Takahara, S.Tasaki, Macromolecules 36 (2003) 6824.

[40] M.Rubinstein, R.H.Colby, Polymer Physics, OUP, Oxford, 2003.

[41] S.H.Zhang, X.Jin, P.C.Painter, J.Runt, Macromols. 36 (2003) 5710.

[42] A.Hariharan, S.K.Kumar, T.P.Russell, Macromolecules 24 (1991) 4909.

[43] C.J.Powell, M.P.Seah, J. Vac. Sci. Technol. A 8 (1990) 735.

[44] G.Beamson, D.Briggs, Surf. Interface Anal. 26 (1998) 343.

[45] U.Gelius, B.Wannberg, P.Baltzer, H.Fellner-Feldegg, G.Carlsson, C.-G.Johansson, J.Larsson, P.Munger, G.Vegerfors, J. Electron Spectrosc. Relat. Phenom. 52 (1990) 747.

[46] G.Beamson, D.Briggs, I.W.Fletcher, D.T.Clark, J.Howard, U.Gelius, B.Wannberg, P.Baltzer, Surf. Interface Anal. 15 (1990) 541.

[47] B.Wannberg, VG Scienta Instruments, Uppsala, Sweden, personal communication.

[48] M.P.Seah, G.C.Smith, in: D.Briggs, M.P.Seah (Eds.), Practical Surface Analysis, vol. 1, second ed., John Wiley, Chichester, 1992, 535.

[49] ESCA300 Instrument manual, Scienta Instruments AB, Uppsala, 1988.

[50] www.casaxps.com.

[51] R.A.L.Jones, L.J.Norton, E.J.Kramer, R.J.Composto, R.S.Stein, T.P.Russell, A.Mansour, A.Karim, G.P.Felcher, M.H.Rafailovich, J.Sokolov, X.Zhao, S.A.Schwarz, Europhys. Lett. 12 (1990) 41.

[52] P.J.Cumpson, Surf. Interface Anal. 31 (2001) 23.

[53] D.Fylstra, L.Lasdon, J.Watson, A.Waren, Interfaces 28 (1998) 29.

[54] E.J.Billo, Excel for Chemists: A Comprehensive Guide, second ed., Wiley-VCH, 2001.

[55] S.Reich, Y.Cohen, J. Polym. Sci. Polym. Phys. Ed. 19 (1981) 1255.

[56] K.Tanaka, A.Takahara, T.Kajiyama, Macromolecules 29 (1996) 3232.

[57] B.Zhang Newby, R.J.Composto, Macromolecules 33 (2000) 3274.

[58] B.Zhang Newby, K.Wakabayashi, R.J.Composto, Polymer 42 (2001) 9155.

[59] Y.Liao, J.You, T.Shi, L.An, P.K.Dutta, Langmuir 23 (2007) 11107.

[60] M.Meloun, T.Syrovy, S.Bordovska, A.Vrana, Anal. Bioanal. Chem. 387 (2007) 941.

**Table 1.**

| **Polymer** | **MW (kDa)** | **MW / Mn** |
|---|---|---|
| PST | 0.8 | 1.17 |
| PST | 2.5 | 1.01 |
| PST | 4.1 | 1.01 |
| PST | 19.3 | 1.07 |
| PST | 289 | 2.20 |
| PVEE | 3.8 | |

MW /Mn = weight average molecular weight / number average molecular weight, i.e. the molecular weight dispersion.

**Table 2. ARXPS curve fit parameters and $\chi$ parameter as a function of PST MW and film thickness.**

| | | | | | | | |
|---|---|---|---|---|---|---|---|
| **PST MW = 0.8 kDa.** | | | | | | | |
| d (nm) | 300 | 150 | 90 | 80 | 25 | 15 | 10 |
| $\phi_b$ | 0.50 (0.02) | 0.49 (0.02) | 0.52 (0.04) | 0.47 (0.02) | 0.42 (0.03) | 0.41 (0.02) | 0.44 (0.03) |
| $\Delta$ (nm) | 0.00 (0.00) | 0.00 (0.00) | 0.45 (1.11) | 0.00 (0.00) | 0.33 (1.02) | 0.89 (0.15) | 0.86 (0.07) |
| $\sigma$ (nm) | 1.54 (0.19) | 1.60 (0.17) | 1.04 (1.34) | 1.74 (0.13) | 1.83 (0.97) | 1.21 (0.38) | 0.53 (0.58) |
| $\chi$ | 0.155 | 0.153 | 0.158 | 0.150 | | | 0.133 |
| **PST MW = 2.5 kDa.** | | | | | | | |
| d (nm) | 260 | 105 | 95 | 25 | 20 | 15 | |
| $\phi_b$ | 0.52 (fixed) | 0.52 (0.03) | 0.47 (0.05) | 0.40 (0.04) | 0.34 (0.06) | 0.24 (0.04) | |
| $\Delta$ (nm) | 2.02 (0.04) | 2.02 (0.18) | 2.08 (0.14) | 2.11 (0.17) | 1.95 (0.14) | 1.76 (0.20) | |
| $\sigma$ (nm) | 1.22 (0.25) | 1.19 (0.43) | 2.28 (0.92) | 1.44 (0.48) | 2.11 (0.95) | 3.11 (0.70) | |
| $\chi$ | 0.067 | 0.067 | 0.066 | 0.064 | 0.065 | 0.070 | |
| **PST MW = 4.1 kDa.** | | | | | | | |
| d (nm) | 305 | 100 | 80 | 25 | 15 | | |
| $\phi_b$ | 0.52 (fixed) | 0.52 (fixed) | 0.52 (fixed) | 0.38 (0.06) | 0.19 (0.13) | | |
| $\Delta$ (nm) | 3.54 (0.09) | 3.34 (0.07) | 3.00 (0.06) | 2.94 (0.34) | 2.86 (0.34) | | |
| $\sigma$ (nm) | 2.94 (0.50) | 2.31 (0.50) | 1.61 (0.34) | 2.15 (0.77) | 2.95 (1.37) | | |
| $\chi$ | 0.052 | 0.051 | 0.050 | 0.050 | | | |

Figures in brackets are standard deviations; d is the blend film thickness; $\phi_b$ = 0.52 (fixed) indicates that it was fixed at 0.52 during the Solver optimisation. $\chi$ parameters are calculated from the values of $\phi_b$, $\Delta$ and $\sigma$, with $\phi_s$ = 1 using equation (7). Where no $\chi$ value is shown this indicates a failure to numerically solve equation (7) indicating a result close to the limit of miscibility.

**Figure 1. C 1s spectra at θ = 90°. a) PST. b) PVEE.**

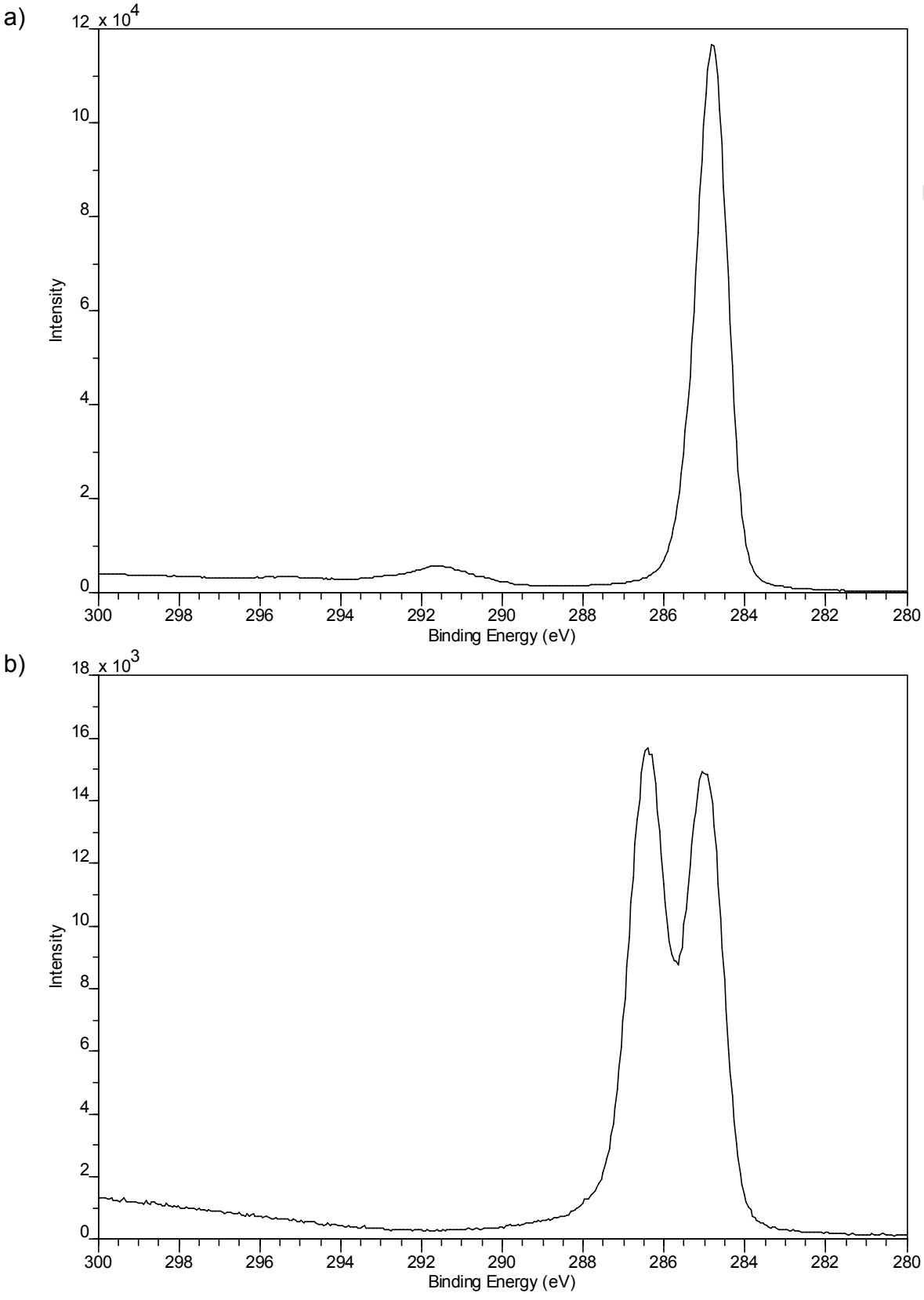

**Figure 2. Angle resolved C 1s spectra for a PST(4.1 kDa) / PVEE(3.8 kDa) blend film ~ 305 nm thick.**

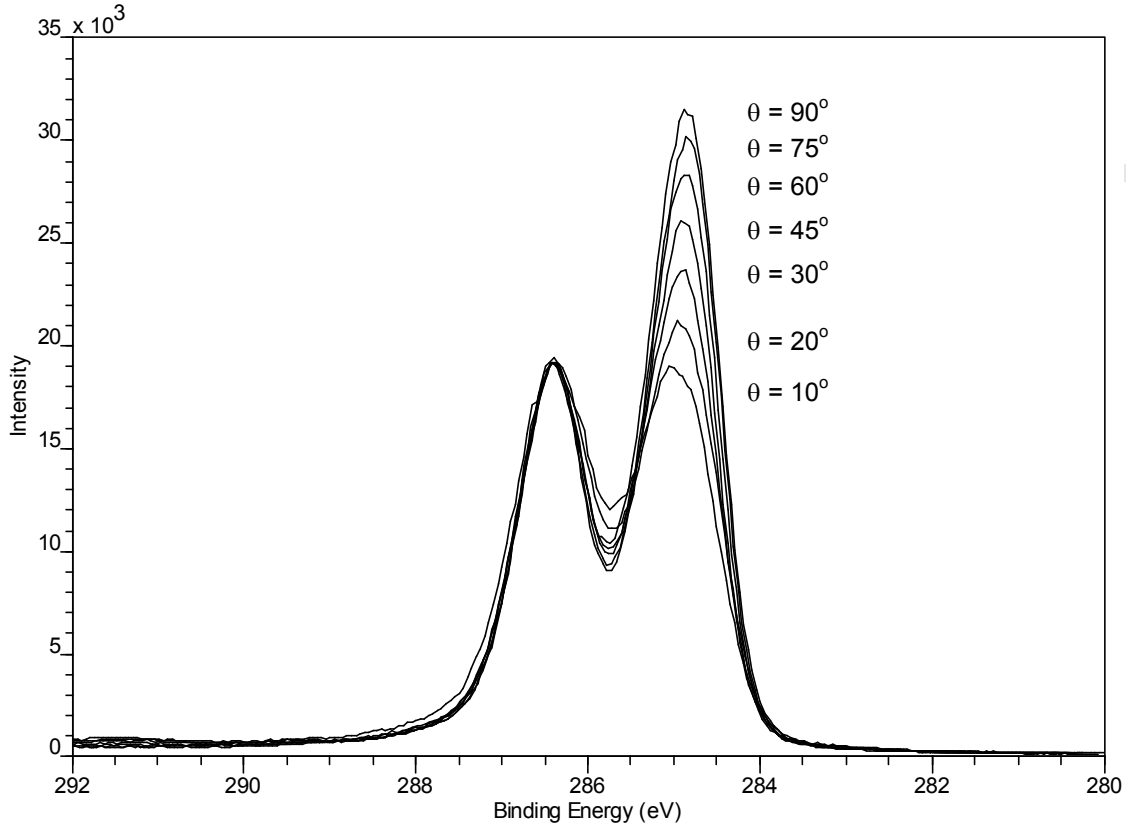

**Figure 3. C 1s curve fit for a PST(4.1 kDa) / PVEE(3.8 kDa) blend film ~ 305 nm thick, θ = 90°.**

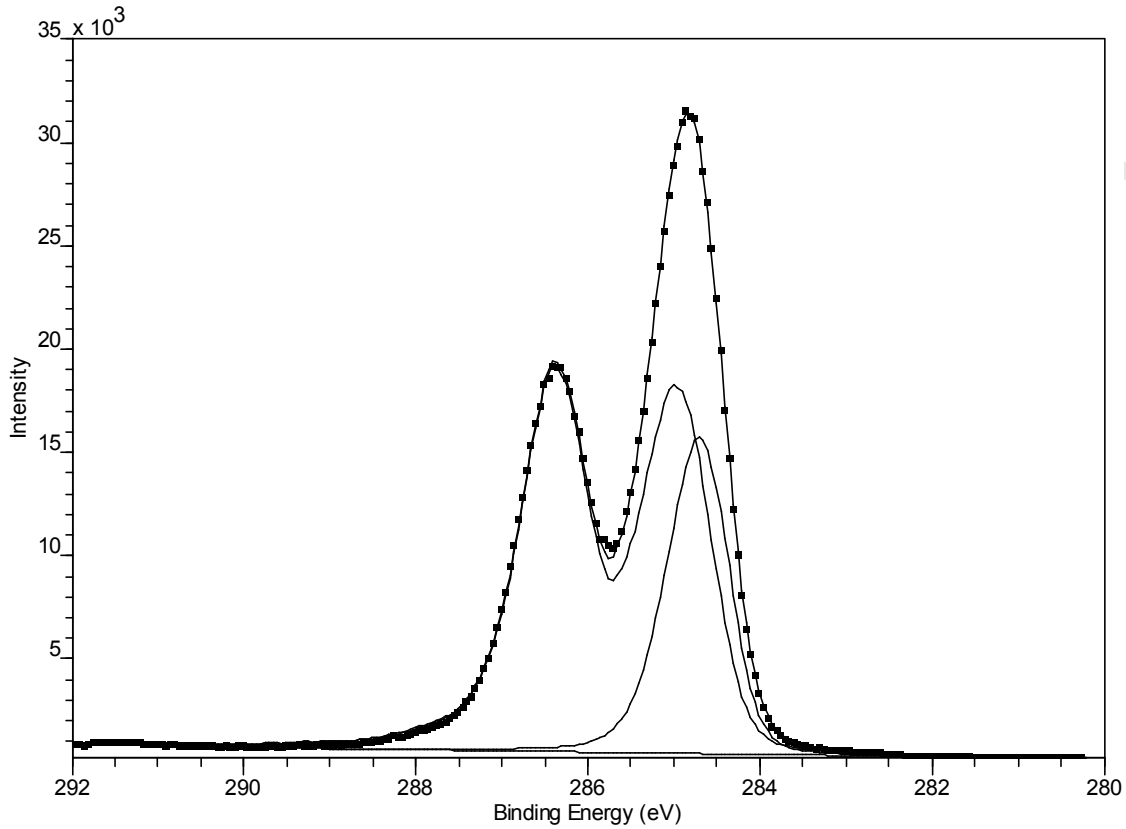

**Figure 4. A hyperbolic tangent CDP.**

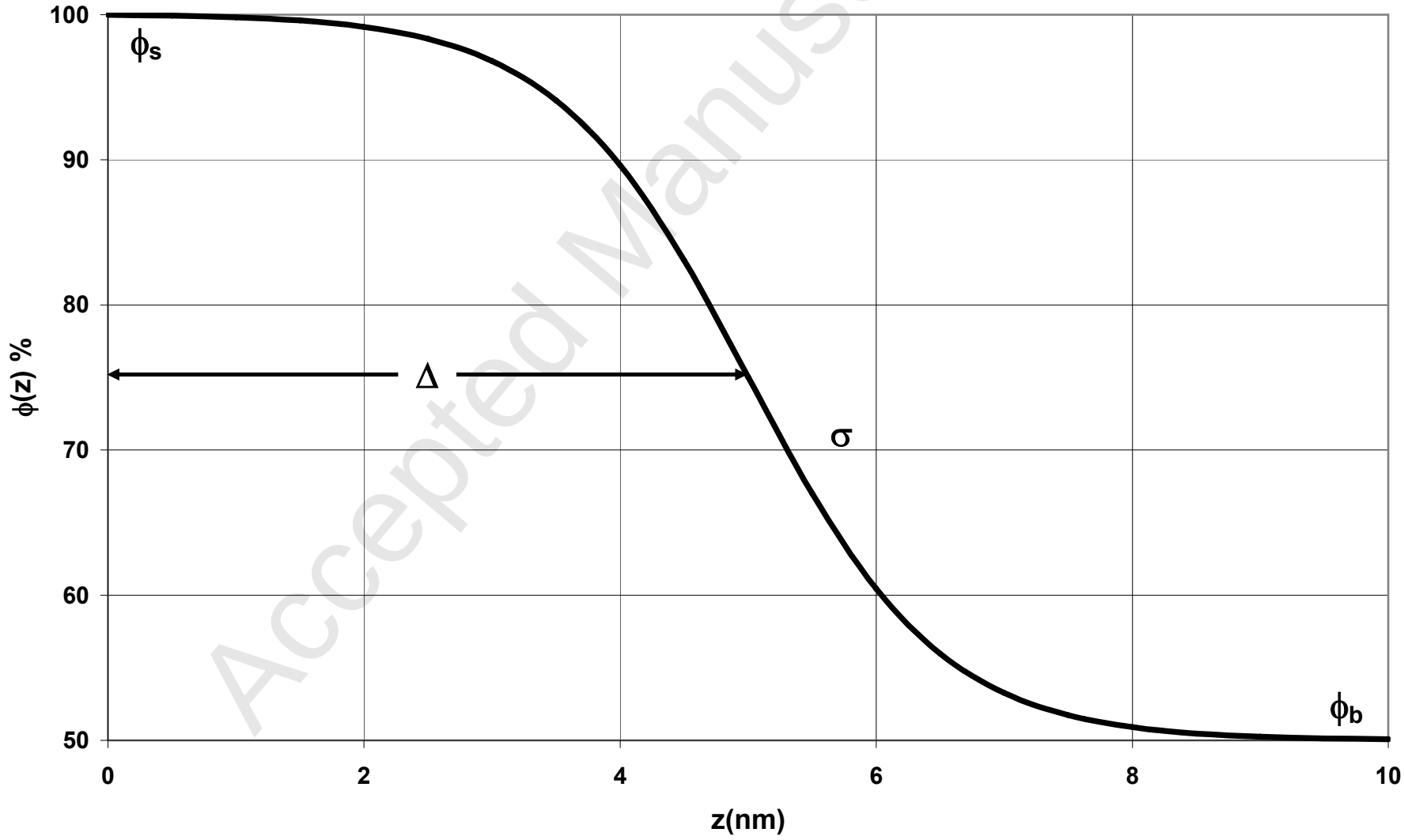

**Figure 5. Angle resolved profiles for PST(0.8 kDa) / PVEE(3.8 kDa), blend films. a) Experimental points and least squares fit lines. b) Hyperbolic tangent CDPs corresponding to a).**

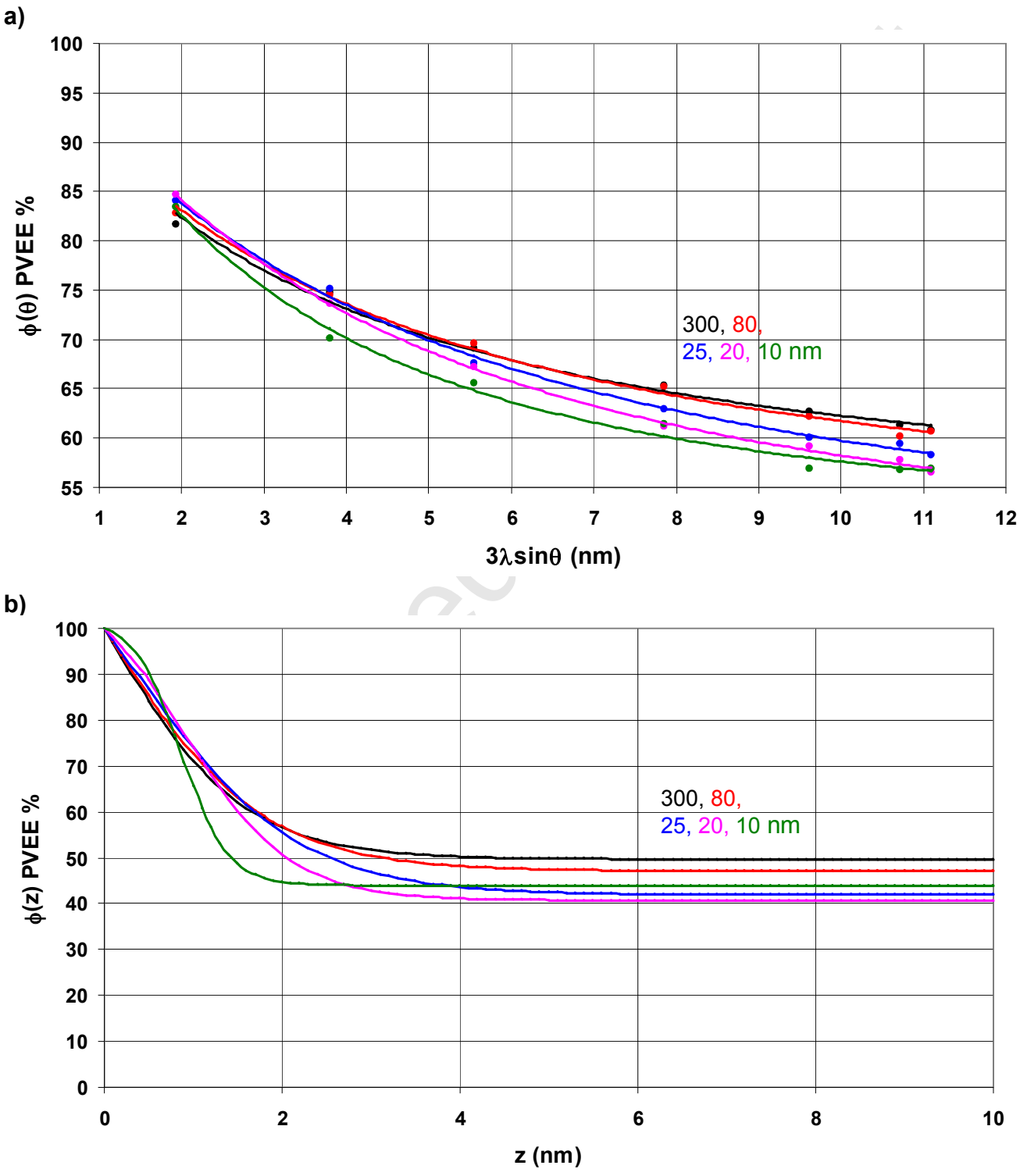

**Figure 6. Angle resolved profiles for PST(2.5 kDa) / PVEE(3.8 kDa), blend films. a) Experimental points and least squares fit lines. b) Hyperbolic tangent CDPs corresponding to a).**

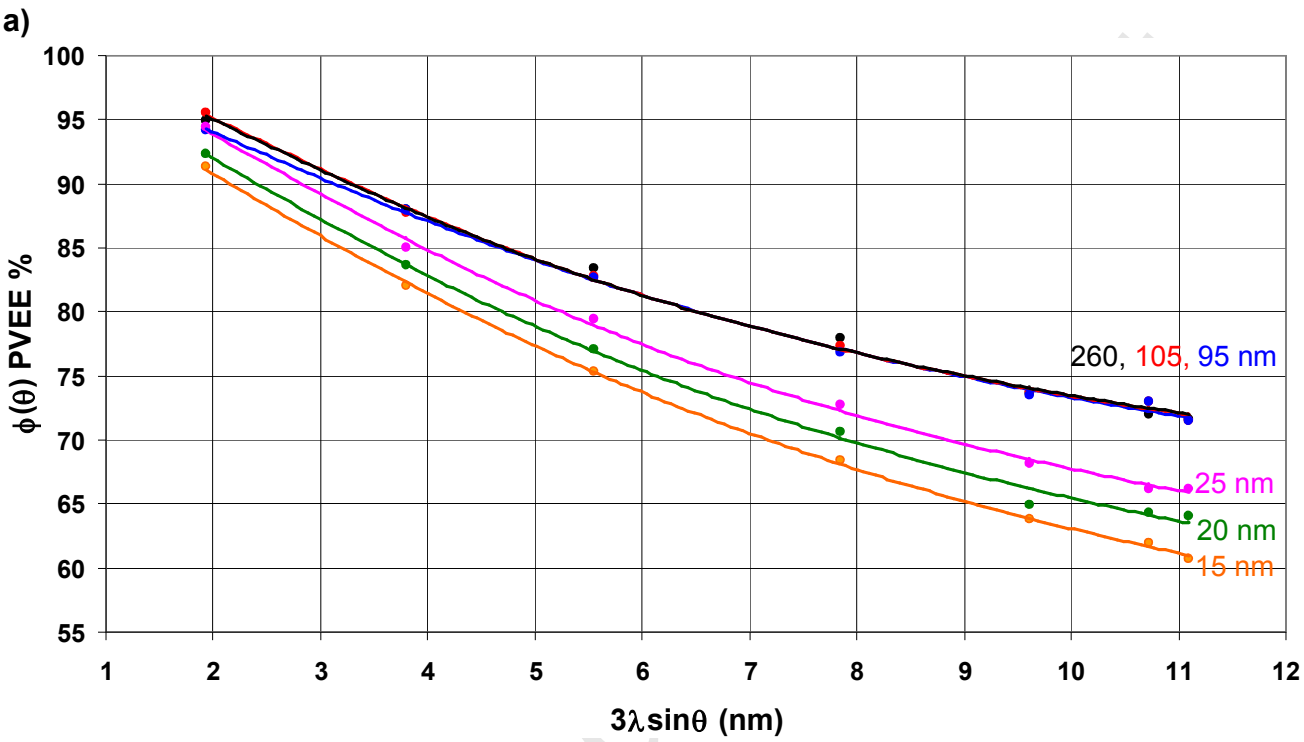


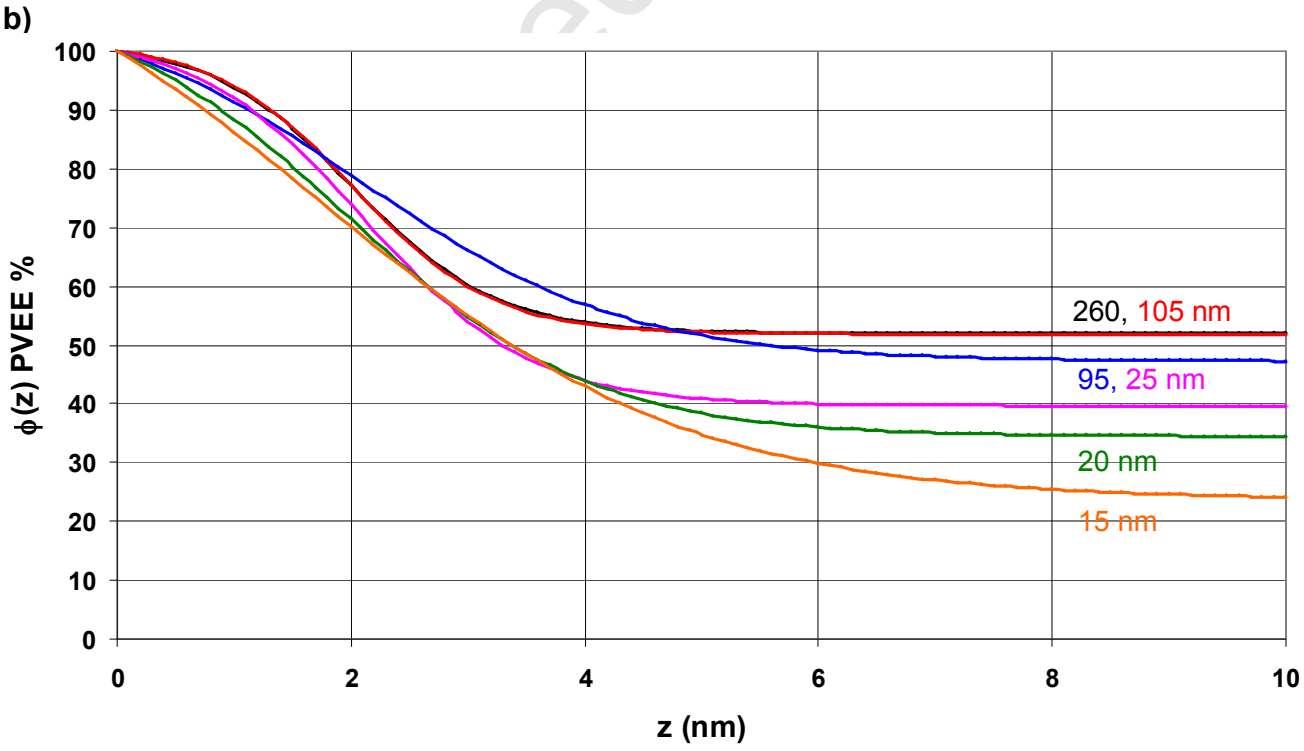

**Figure 7. Angle resolved profiles for PST(4.1 kDa) / PVEE(3.8 kDa), blend films. a) Experimental points and least squares fit lines. b) Hyperbolic tangent CDPs corresponding to a).**

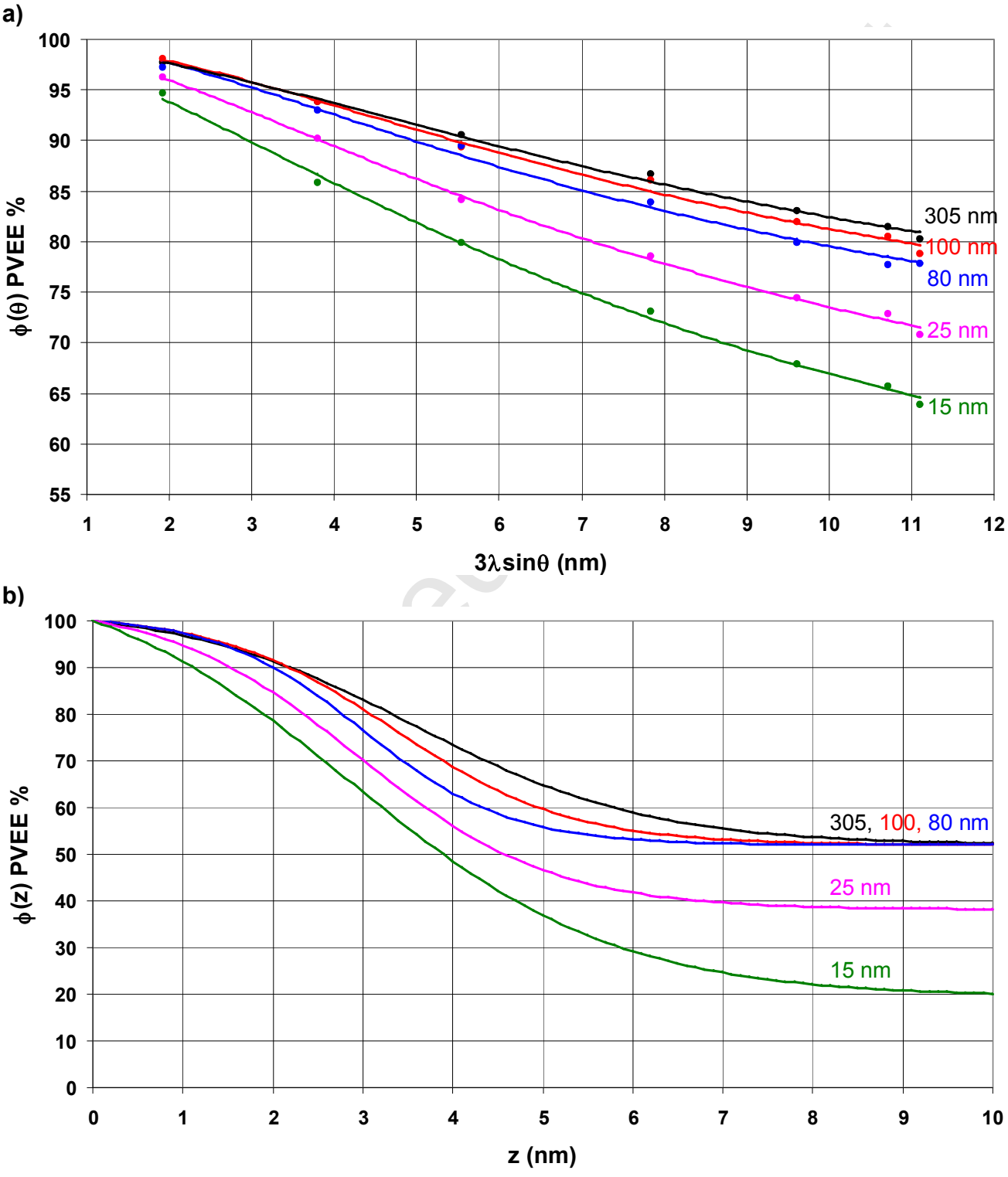

**Figure 8. SFM topography images. a) PST(0.8 kDa) / PVEE(3.8 kDa). b) PST(289 kDa) / PVEE(3.8 kDa).**

**a)**

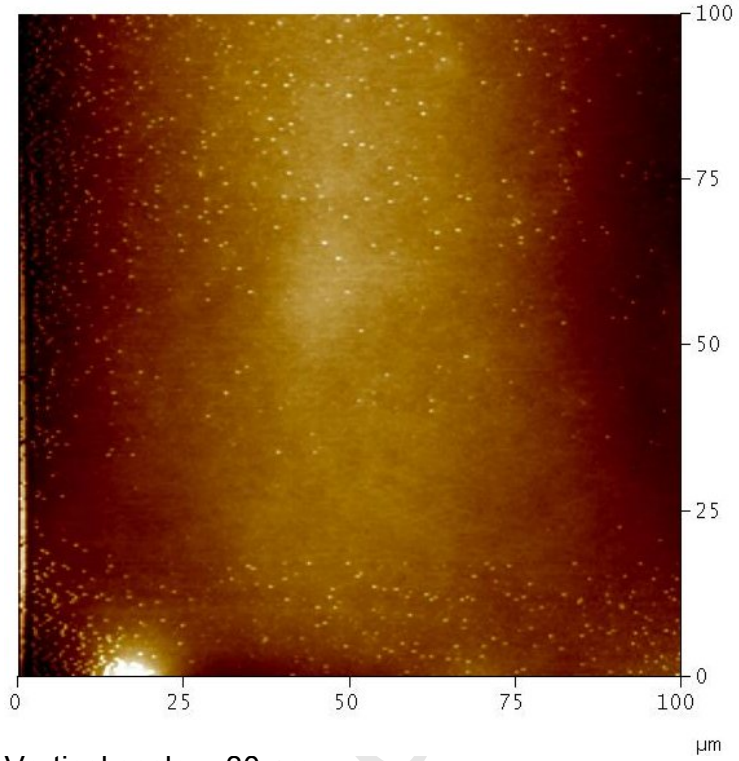


Vertical scale = 30 nm.

Film thickness ~ 90 nm.

RMS roughness = 0.6 nm.

**b)**

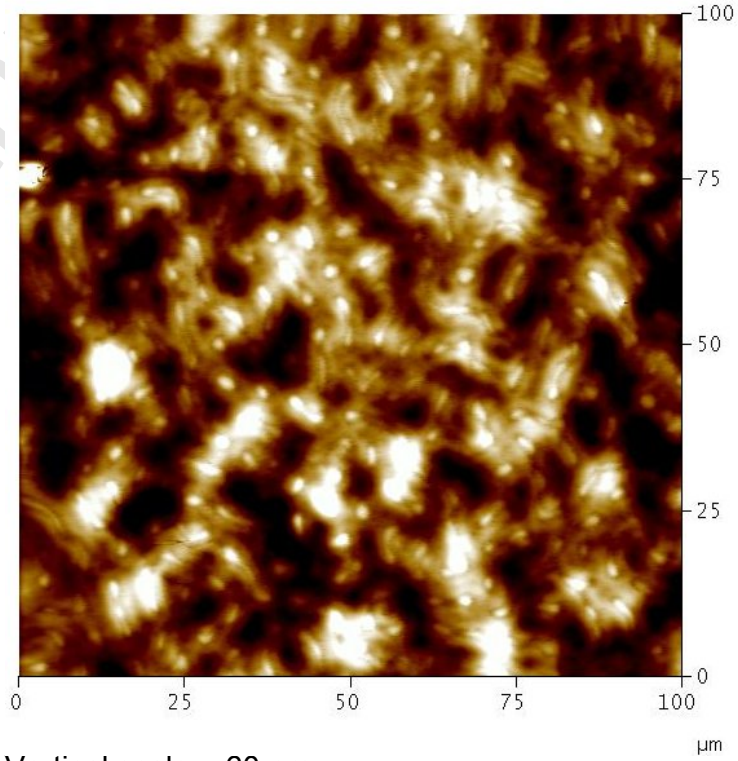


Vertical scale = 60 nm.

Film thickness ~ 120 nm.

RMS roughness = 11.7 nm.